MOLECULAR AND CELLULAR BIOLOGY, June 1997, p. 3429–3439 Vol. 17, No. 6
0270-7306/97/$04.00+0

Saccharomyces cerevisiae Mpt5p Interacts with Sst2p and Plays Roles in Pheromone Sensitivity and Recovery from Pheromone Arrest

TAOSHENG CHEN† AND JANET KURJAN*

Department of Microbiology and Molecular Genetics, Cell and Molecular Biology Program, and Vermont Cancer Center, College of Medicine and College of Agriculture and Life Sciences, University of Vermont, Burlington, Vermont 05405-0068

Received 30 January 1996/Returned for modification 9 April 1996/Accepted 13 March 1997

***SST2* plays an important role in the sensitivity of yeast cells to pheromone and in recovery from pheromone-induced G_1 arrest. Recently, a family of Sst2p homologs that act as GTPase-activating proteins (GAPs) for Gα subunits has been identified. We have identified an interaction between Sst2p and the previously identified Mpt5p by using the two-hybrid system. Loss of Mpt5p function resulted in a temperature-sensitive growth phenotype, an increase in pheromone sensitivity, and a defect in recovery from pheromone-induced G_1 arrest, although the effects on pheromone response and recovery were mild in comparison to those of *sst2* mutants. Overexpression of either Sst2p or Mpt5p promoted recovery from G_1 arrest. Promotion of recovery by overexpression of Mpt5p required Sst2p, but the effect of overexpression of Sst2p was only partially dependent on Mpt5p. Mpt5p was also found to interact with the mitogen-activated protein kinase homologs Fus3p and Kss1p, and an *mpt5* mutation was able to suppress the pheromone arrest and mating defects of a *fus3* mutant. Because either *mpt5* or *cln3* mutations suppressed the *fus3* phenotypes, interactions of Mpt5p with the G_1 cyclins and Cdc28p were tested. An interaction between Mpt5p and Cdc28p was detected. We discuss these results with respect to a model in which Sst2p plays a role in pheromone sensitivity and recovery that acts through Mpt5p in addition to a role as a Gα GAP suggested by the analysis of the Sst2p homologs.**

The yeast *Saccharomyces cerevisiae* has two haploid cell types, **a** and α, which mate to produce the **a**/α diploid. **a** and α cells secrete the peptide pheromones **a**- and α-factor, respectively, which bind and activate specific receptors on cells of the opposite mating type (reviewed in references 41 and 48). Response to pheromone results in the transcriptional activation of a set of genes, morphological changes, and cell cycle arrest in G_1.

Pheromone response occurs through a highly conserved pathway. The **a**- and α-factor receptors Ste3p and Ste2p, respectively, act through a heterotrimeric G-protein composed of Gpa1p (α), Ste4p (β), and Ste18p (γ) subunits (20, 50, 70). In this pathway, free βγ activates the downstream pathway. This downstream pathway involves several kinases, including Ste20p (42, 58) and members of a mitogen-activated protein (MAP) kinase cascade, Ste11p (MAP kinase kinase kinase), Ste7p (MAP kinase kinase), and the functionally redundant MAP kinase homologs, Fus3p and Kss1p (reviewed in reference 44). Recent results have suggested that Ste5p acts as a scaffold for components of the MAP kinase cascade (11, 47, 57). The transcription factor Ste12p acts downstream of the MAP kinase cascade to induce pheromone-responsive genes (26, 31, 65). Fus3p also phosphorylates and activates Far1p (32, 55, 67), which inactivates Cln1p-Cdc28p and Cln2p-Cdc28p activity, leading to cell cycle arrest in G_1 (56).

Growth arrest after exposure of cells to pheromone is transient; after a time, cells resume growth through a process known as desensitization or recovery (7, 8, 51). Several components of the pheromone response pathway, including the pheromone receptors, G-protein subunits, and the MAP kinase homolog Kss1p, have been implicated in desensitization (reviewed in reference 41).

An important role for the *SST2* gene in desensitization was originally indicated by mutant phenotypes (7, 8); *sst2* mutations result in a >100-fold increase in sensitivity to pheromone, which is referred to as supersensitivity, and a defect in recovery from pheromone arrest. *sst2* mutations have similar effects in **a** and α cells, and Sst2p acts in a cell-intrinsic manner. *SST2* expression is haploid specific and pheromone inducible (21). Recently, a family of proteins with sequence similarity to Sst2p has been identified in nematodes and mammals (reviewed in references 24 and 37). Members of the mammalian family have been shown to act as GTPase-activating proteins for Gα subunits, consistent with indications that Sst2p may act at the level of Gpa1p (22, 23). In this paper, we characterize the role for the Sst2p-interacting protein Mpt5p and discuss implications for Sst2p function.

MATERIALS AND METHODS

Strains. The *MAT*α strain N435-2A (*his7 lys7 met6 arg1 gal4*) was used for the mating assays. The two-hybrid assays were done with strains Y190 (*MAT***a** *leu2-3,112 ura3-52 trp1-901 his3-Δ200 ade2-101 gal4Δ gal80Δ GAL-lacZ GAL-HIS3 cyh*^{r}) and Y187 (*MAT*α *leu2-3,112 ura3-52 trp1-901 his3-Δ200 ade2-101 gal4Δ gal80Δ GAL-lacZ met*$^-$), both of which were provided by S. Elledge, or with Y187 with a *far1::ADE2* deletion to prevent growth defects resulting from some of the two-hybrid constructs containing fusions to components of the pheromone response pathway. All other *S. cerevisiae* strains used were isogenic to W303-1A (*MAT***a** *ade2-1 can1-100 ura3-1 leu2-3,112 trp1-1 his3-11,15*). The disruption strains used were RAK40 (*sst2::HIS3*), TCK9 (*kss1::HIS3*), RAK29 (*fus3::LEU2*), TCK21 (*far1::ADE2*), TCK13 (*mpt5::HIS3*), TCK14 (*mpt5::URA3*), TCK19 (*mpt5::URA3 sst2::HIS3*), TCK24 (*mpt5::HIS3 fus3::LEU2*), TCK31 (*cln3::URA3*), TCK28 (*fus3::LEU2 cln3::URA3*), and TCK25 (*mpt5::HIS3 far1::ADE2*). *Escherichia coli* TG-1 was used for plasmid analysis and subcloning.

* Corresponding author. Mailing address: Department of Microbiology and Molecular Genetics, University of Vermont, Burlington, VT 05405-0068. Phone: (802) 656-8024. Fax: (802) 656-8749. E-mail: jkurjan@zoo.uvm.edu.

† Present address: Department of Microbiology, University of Virginia Health Sciences Center, Charlottesville, VA 22908.

TABLE 1. Oligonucleotides used in this study

Oligonucleotide[a]	Gene	Sequence[b]	Restriction site
1U	*SST2*	5′-AGATAGAGTTGTA**CC**ATGGTGGATA-3′	*Nco*I
1D		5′-GAGTAAGACTCT**GG**AT**CC**AATTAGC-3′	*Bam*HI
2M		5′-CTATCTGAGGCGTTA**A**GG**C**TTCAA-3′	*Hin*dIII
3U	*MPT5*	5′-CGGGATCTTCTAACAACAAATAGC-3′	
3D		5′-GGAGGATTTTGGATACGTGTTCGG-3′	
4U		5′-TCAAATAACTCC**CAT**ATGTCTTACA-3′	*Nde*I
5U		5′-CCGCCTTTGGGCCA**T**ATGAAT-3′	*Nde*I
6U67		5′-CAAC**CAT**G**G**ATTCTGCTAAC-3′	*Nco*I
6U362		5′-AAA**CCA**T**GG**TAAGCGTTTG-3′	*Nco*I
6U569		5′-AAG**CCA**T**G**GCTTATGCAGAAGC-3′	*Nco*I
6D		5′-AAA**CT**CG**AG**TTATGGCAAAGTG-3′	*Xho*I
7M		5′-TTGGAGCCCGTG**G**CCCCTCCG-3′	
10U		5′-AATGCTGCTAGCAACTCC-3′	*Nhe*I
FLAG		5′-CCGCTCGAGTTACTTGTCATCGTCATCCTTGTAGTCTGGCAAAGTGAATTG-3′	*Xho*I
8U	*STE21*	5′-GGAAGAAAAAG**CC**ATGGATTCC-3′	*Nco*I
8D		5′-GGCACCT**CGAG**ATCAGTTGTC-3′	*Xho*I
9U	*CDC28*	5′-TT**C**GACCATG**G**GCGGTGAATTAGC-3′	*Nco*I
9D		5′-GATTA**GG**AT**C**CTTATGATTCTTGG-3′	*Bam*HI
H1	HA1 tag	5′-GATGTACCCATACGACGTCCCAGACTACGCTACTAGTGCCATGGACCA-3′	*Spe*I, *Nco*I
H2		3′-CGCTACATCGGTATGCTGCAGGGTCTGATGCGATGATCACGGTACCTGGTAT-5′	

[a] U represents the upstream oligonucleotide and D indicates the downstream oligonucleotide used for PCR mutagenesis; M indicates a mutagenic oligonucleotide, and H1 and H2 are a complementary oligonucleotide pair used to insert an HA1 epitope tag.

[b] Bold letters indicate nucleotides that differ from the wild-type sequence; single underlines indicate the resulting restriction sites, double underlines indicate an ATG initiation codon in upstream oligonucleotides or a termination codon in the reverse strand of downstream oligonucleotides, and a dotted underline indicates an epitope tag sequence (HA or FLAG).

Two-hybrid screen. All plasmids used in the two-hybrid system and the cDNA library in pACT were provided by S. Elledge (34), and the genomic library in pGAD1, pGAD2, and pGAD3 was provided by S. Fields (10). To construct a Gal4p DNA binding domain (BD)-Sst2p fusion construct, which includes the HA1 epitope tag, the *SST2* open reading frame was amplified by PCR with oligonucleotides 1U and 1D (Table 1). The *Nco*I-*Bam*HI-cleaved PCR product was subcloned into *Nco*I-*Bam*HI-cleaved pAS2 to produce pAS2-*SST2*. pAS2-*SST2* (*TRP1*) was transformed into Y190 and shown not to activate the Gal4p-regulated *lacZ* reporter gene. Expression of the fusion protein was confirmed by Western blot analysis of yeast extracts with antibody against the HA1 epitope (data not shown).

Y190[pAS2-*SST2*] was transformed with the yeast cDNA and genomic libraries (*LEU2*) of activation domain (AD) fusions. About 10^7 transformants from each library were plated on medium lacking leucine and tryptophan to select for the plasmids and lacking histidine but containing 25 mM 3-aminotriazole (Sigma) to enrich for colonies in which BD-Sst2p and an interacting AD fusion allow growth due to expression of the Gal4p-regulated *HIS3* gene (34). His^+ colonies were screened for β-galactosidase activity by a colony lift assay (5). Blue colonies, which appeared at times varying from 30 min to overnight, were analyzed further.

To test the specificity of the interactions, the His^+ colonies were streaked on leucineless plates to allow the loss of pAS2-*SST2*, crossed to α strains containing several BD fusions, and tested for activation of the *lacZ* reporter gene (34). In addition, AD fusion plasmids were recovered in *E. coli*, transformed into haploid strains (Y187 or Y190) along with BD-Sst2p or the control fusions, and tested for *GAL-lacZ* activation.

Construction of *mpt5* disruptions and deletions. Transposon mutagenesis was performed as described previously (21, 63). The 0.9-kb *Xho*I fragment from the original AD-Mpt5p[64–362] plasmid was subcloned into the pHSS20 vector (provided by S. Siefert) and subjected to insertional mutagenesis with a Tn*3*::*URA3* minitransposon. Plasmids arising from independent groups of transpositions were pooled, linearized with *Not*I, and transformed into the **a** strain W303-1A. Ura^+ transformants were tested for a phenotype, and gene replacements were confirmed by Southern analysis. To obtain α *mpt5*::*URA3* disruption mutants, the **a** *mpt5*::*URA3* disruption mutants were transformed with a p*GAL-HO* plasmid (36), grown on galactose to allow mating-type switching, plated on glucose, and tested for mating.

The *mpt5*::*HIS3* disruption plasmid was constructed by inserting a *HIS3* *Bam*HI fragment into the *Bgl*II site in *MPT5*, resulting in an insertion at amino acid 188 of the open reading frame. The *mpt5*::*ADE2* deletion plasmid was constructed by replacing a 1.9-kb *Nhe*I-*Bsg*I fragment within *MPT5* with a *Bgl*II *ADE2* fragment by blunt-end ligation, resulting in deletion of amino acids 79 to 713 of the 834-amino-acid open reading frame. These fragments were used for one-step gene replacements in W303-1A and W303-1B (60).

Plasmid constructions for overexpression studies. To allow the expression of *SST2* under the *PGK* promoter, a *Hin*dIII site was constructed 30 bp upstream of the *SST2* ATG initiation codon by site-directed mutagenesis (72) with oligonucleotide 2M (Table 1). The resulting 3.6-kb *Hin*dIII *SST2* fragment was subcloned into the *Hin*dIII site of the YEp*PGK* vector (38) to produce YEp*PGK-SST2*.

The AD-Mpt5p[64–362] plasmid isolated in the two-hybrid screen contained a 0.9-kb *Xho*I fragment from within *MPT5*. This fragment was labeled with [α-^{32}P]dCTP by using an oligolabeling kit (Pharmacia) and used to screen the genomic pGAD libraries (10) by hybridization to obtain the intact *MPT5* gene. DNA sequencing determined that the sequence was identical to the sequences in the databases (accession no. D25541 and D26184).

An *MPT5* fragment, including about 600 bp upstream of the initiation codon and 200 bp downstream of the termination codon, was amplified from a pGAD-*MPT5* plasmid with oligonucleotides 3U and 3D (Table 1) and subcloned into *Srf*I-cleaved pCR-ScriptSK(+) (Stratagene) by blunt-end ligation to create pCR2-*MPT5*. A *Sac*I-*Xho*I fragment of pCR2-*MPT5* was subcloned into the *Sac*I-*Xho*I sites of pRS425 and pRS315 (12, 64) to create YEp-*MPT5* and YCp-*MPT5* plasmids, respectively, with *MPT5* expressed from its own promoter.

To express *MPT5* under the control of the *PGK* promoter, pPGA1 (*LEU2*) (62) was first modified; the unique *Acc*I site was replaced with a *Xho*I linker to produce pPGAX, and the 0.7-kb *Eco*RV-*Bst*EII fragment from within *LEU2* in pPGAX was replaced with a 1.6-kb *TRP1* *Nae*I-*Aat*II fragment from pRS304 (64) to produce pPGAW. The *MPT5* open reading frame was amplified by PCR with oligonucleotides 4U and 3D (Table 1) and subcloned into *Srf*I-cleaved pCR-ScriptSK(+) to create pCR1-*MPT5*. To create YEp*PGK-MPT5*, a *Sac*I-*Xho*I fragment from pCR1-*MPT5* (the *Sac*I site is within the multiple-cloning site of the vector, 40 bp upstream of the *MPT5* initiation codon) was subcloned into *Sac*I-*Xho*I-cleaved pPGAW. The *Sac*I-*Xho*I fragment from pPGAW was deleted to produce pPGAWΔ, which was used as a control vector. To make the *MPT5[29–834]* construct, oligonucleotides 5U and 3D were used for PCR amplification and the fragment was subcloned into *Srf*I-cleaved pCR-ScriptSK(+) to create pCR-*MPT5[29–834]*. The *Sac*I-*Xho*I fragment of this construct was then subcloned into *Sac*I-*Xho*I-cleaved pPGAW to create YEp*PGK-MPT5[29–834]*.

Construction of Mpt5p plasmids for two-hybrid assays. The Gal4p AD and BD fusions to intact Mpt5p were constructed by subcloning the *Nco*I-*Xho*I fragment from pCR1-*HA-MPT5* (see below) into *Nco*I-*Xho*I-cleaved pACTII and pAS2, respectively (34). The BD-Mpt5p construct gave strong activation of

the *GAL4-lacZ* reporter gene; therefore, the assays were done with AD-Mpt5p constructs.

AD fusions in pACTII to various portions of Mpt5p were constructed. AD-Mpt5p[1–234] was created by deleting an internal *Bam*HI fragment from AD-*MPT5*. AD-Mpt5p[29–834] was created by subcloning the *Nde*I-*Xho*I fragment from pCR-*MPT5[29–834]* into *Nde*I-*Xho*I-cleaved pACTII. To create AD-Mpt5p[1–569], an internal *Hin*dIII fragment from pCR1-*MPT5* was deleted and the *Nde*I-*Xho*I fragment from the resulting plasmid was subcloned into *Nde*I-*Xho*I-cleaved pACTII. AD-Mpt5p[234–834] was created by subcloning a *Bam*HI fragment from pCR1-*MPT5* into *Bam*HI-cleaved pACT-*MPT5*[64–362], the original isolate from the two-hybrid screen.

AD-Mpt5p[67–834], AD-Mpt5p[362–834], and AD-Mpt5p[569–834] were created by amplifying fragments from pRS315-*MPT5* by PCR with the upstream oligonucleotides 6U67, 6U362, and 6U569, respectively, and the downstream oligonucleotide 6D (Table 1). The *Nco*I-*Xho*I-digested PCR products were subcloned into *Nco*I-*Xho*I-cleaved pACTII to produce AD-Mpt5p[67–834], AD-Mpt5p[362–834], and AD-Mpt5p[569–834].

Other constructions for two-hybrid assays. BD-Ste20p (pKB84.7), BD-Ste5p (pSL2019), BD-Ste11p (pSL2121), and BD-Ste7p (pSL1962) were provided by J. A. Printen and G. F. Sprague (57). BD-Gpa1p (pAS2-*GPA1*) was created by subcloning a 1.8-kb *Nco*I-*Bam*HI fragment from pSK-OM1A, which has an *Nco*I site at the initiation codon of *GPA1* (provided by S. DeSimone), into *Nco*I-*Bam*HI-cleaved pAS2. BD-Fus3p was created by subcloning the 1.1-kb *FUS3* *Bam*HI fragment from pSL2175 (57) into *Bam*HI-cleaved pAS2. BD-Kss1p was created by subcloning the 1.1-kb *KSS1* *Bam*HI fragment from pSL2120 (57) into *Bam*HI-cleaved pAS2. To create BD-Ste21p, the *STE21* open reading frame (1) was amplified by PCR from p316-12 (provided by R. Akada) with oligonucleotides 8U and 8D (Table 1); the *Nco*I-*Xho*I-digested PCR product was subcloned into *Nco*I-*Sal*I-cleaved pAS2. To create BD-Cdc28p, the *CDC28* open reading frame was amplified by PCR from yeast genomic DNA with oligonucleotides 9U and 9D (Table 1); the *Nco*I-*Bam*HI-digested PCR product was subcloned into *Nco*I-*Bam*HI-cleaved pAS2.

Plasmid constructions for biochemical assays. Mpt5p with an N-terminal epitope tag (HA) was produced by annealing oligonucleotides H1 and H2 (Table 1) and ligating the resulting fragment into *Sac*II-*Nde*I-cleaved pCR1-*MPT5* to create pCR1-*HA-MPT5*. To construct a glutathione *S*-transferase–Mpt5p fusion (GST-Mpt5p), the *Nco*I-*Hin*dIII fragment from pCR1-*HA-MPT5* was subcloned into *Nco*I-*Hin*dIII-cleaved pEG(KG) (49) to give a GST-Mpt5p fusion expressed under galactose control (p*GAL-MPT5*). Mpt5p with a C-terminal epitope tag (FLAG) was produced with oligonucleotides 10U and FLAG (Table 1) to amplify *MPT5* by PCR with YEp-*MPT5* as a template. The PCR amplification product was cleaved with *Nhe*I and *Xho*I and used to replace the corresponding *Nhe*I-*Xho*I fragment in YEp-*MPT5* to produce YEp-*MPT5-FLAG*. To construct epitope-tagged Sst2p, the *Nco*I-*Hin*dIII fragment from pAS2-*SST2* was used to replace the *MPT5* sequence in pCR1-*HA-MPT5* to create pCR1-*HA-SST2*. A *Sac*I-*Hin*dIII fragment from pCR1-*HA-SST2* was subcloned into YEp*PGK* to create YEp*PGK-HA-SST2*.

Biochemical assays of Mpt5p interactions. To test for an interaction of Sst2p with Mpt5p, yeast cells (W303-1A) containing YEp*PGK-HA-SST2* and either p*GAL-MPT5* or p*GAL-GST*(pEG[KG]) were grown at 30°C to an optical density at 600 nm (OD_{600}) of 0.6 to 0.8 in 2% raffinose medium selective for the plasmids, collected, resuspended in selective medium with 2% galactose, grown for 4 h, divided in two, and then incubated for an additional 1 h with or without 100 nM α-factor. Yeast extracts were prepared with modified H buffer (25 mM Tris-HCl [pH 7.4], 15 mM EGTA, 15 mM $MgCl_2$, 1 mM dithiothreitol, 0.1% Triton X-100, 1 mM phenylmethylsulfonyl fluoride, 5 μg each of pepstatin A, leupeptin, and aprotinin per ml) containing 10% glycerol (30). Protein concentrations were determined by the Bio-Rad protein assay as specified by the manufacturer. GST or GST-Mpt5p was affinity purified with glutathione-agarose (Sigma) as described by Kranz et al. (40) with a volume of extract containing about 1 mg of yeast protein in 400 μl of modified H buffer containing 150 mM NaCl and 1% bovine serum albumin. Samples were denatured in Laemmli sample buffer, electrophoresed on sodium dodecyl sulfate (SDS)–6% polyacrylamide gels, and transferred to nylon membranes (2). The GST-Mpt5p fusion protein and HA1-tagged Sst2p were detected with the enhanced chemiluminescence (ECL) system (Amersham) as specified by the manufacturer, with mouse monoclonal anti-GST antibody (Santa Cruz) and monoclonal anti-HA antibody 12CA5 (Boehringer Mannheim), respectively, as primary antibodies. Horseradish peroxidase-conjugated anti-mouse immunoglobulin (Amersham) was used as the secondary antibody.

To test for interactions of Mpt5p with Fus3p and Cdc28p, yeast cells (W303-1A) containing either YEp*MPT5-FLAG* or the control plasmid YEp-FLAG-1 BAP (bacterial alkaline phosphatase expressed under the *ADH2* promoter [Kodak]) were grown at 30°C to an OD_{600} of 0.6 to 0.8 in 2% glucose medium selective for the plasmids. Half of each culture was induced with 100 nM α-factor, and yeast extracts were prepared as described above. Volumes of extract containing 300 μg of protein were aliquoted to tubes containing modified H buffer without glycerol to a final volume of 0.5 ml. Then 15 μl of 5 M NaCl and 50 μl of anti-FLAG M2 affinity gel (Kodak) were added, and the extracts were incubated overnight at 4°C with rotation. Immune complexes were pelleted and washed as described by the manufacturer, resuspended in 100 μl of Laemmli buffer, boiled for 5 min, electrophoresed on SDS–10% polyacrylamide gels, and transferred to nylon membranes. Mpt5p-FLAG and the FLAG-BAP control were detected as described above with the mouse monoclonal anti-FLAG antibody M2 (Kodak). Endogenous Fus3p and Cdc28p were detected with rabbit polyclonal anti-Fus3 (Upstate Biotechnology Inc.) and polyclonal anti-Cdc28 antibody 182 (provided by B. Futcher [69]), respectively. Horseradish peroxidase-conjugated anti-mouse (FLAG M2) or anti-rabbit (Fus3p and Cdc28p) immunoglobulins (Amersham) were used as secondary antibodies.

β-Galactosidase assays. Strains were grown to an OD_{600} of 0.2 to 0.5 in medium selective for plasmids and harvested. For pheromone induction, cells were induced with various concentrations of α-factor for 2 h before being harvested. The cells were prepared and permeabilized, ONPG (*o*-nitrophenyl-β-D-galactopyranoside) was used as the substrate, and β-galactosidase units were calculated as described previously (2).

Pheromone response and mating assays. Halo assays to test pheromone response and recovery were performed as described previously (21). Thin lawns of cells (about 5×10^5 mid-log-phase cells) were spread directly onto plates or suspended in 5 ml of soft agar and spread onto plates. α-Factor was spotted either directly onto the nascent lawn or onto sterile filter disks, which were placed on the nascent lawn. The plates were incubated at 30°C, and the zone of growth inhibition was scored. To assay the induction of a pheromone-inducible reporter gene, the *FUS1::lacZ* *Nco*I fragment from pSB234 (66) was subcloned into pYSK136 (YEp-*TRP1* [27]) to construct pTCFL1. pTCFL1 was transformed into the strains to be tested, various concentrations of α-factor were added, cells were incubated for 2 h at 30°C, and β-galactosidase activities were determined. Mating assays were done by replica plating yeast strains onto lawns of tester cells (N435-2A) in 0.3 ml of yeast extract-peptone-dextrose (YEPD) medium on minimal plates and incubating at 30°C for 48 h.

RESULTS

Identification of a protein that interacts specifically with Sst2p. To identify proteins that interact with Sst2p, we used the yeast two-hybrid system (10, 34). A Gal4p BD-Sst2p fusion was able to complement an *sst2* mutation but did not induce reporter gene expression (data not shown), indicating that it maintained function and that it could be used in a two-hybrid screen.

A haploid strain (Y190) expressing BD-Sst2p was transformed with yeast cDNA and genomic libraries expressing fusions to the Gal4p AD. The His^+ $LacZ^+$ clones isolated corresponded to six genes (Table 2) as determined by DNA sequencing of the fusion boundaries of the plasmids followed by database searches. The genes isolated included two novel genes (called *ORF1* and *ORF2*), *RIF1* (33), *CDC23* (25), TyA (13), and a gene that has been called *HTR1* (39) or *MPT5* (accession no. D26184). Because the name *HTR1* had previously been used for a different gene (53), we will refer to this gene as *MPT5*.

The specificity of the interactions with BD-Sst2p was tested by assaying the AD fusion constructs in combination with several BD fusion constructs (4). In **a**/α diploids, all of the constructs showed a specific interaction with BD-Sst2p, with the exception of AD-Orf2p, which also showed an interaction with BD-Snf1p (data not shown). In a haploid strain, however, most of the AD fusions showed an interaction with at least one BD fusion in addition to BD-Sst2p (Table 2). AD-Mpt5p was the only fusion that showed a specific interaction with BD-Sst2p. The AD-Mpt5p isolate contained a 0.9-kb insert from within *MPT5* that could encode amino acids 64 to 362 of the 834-amino-acid open reading frame (15, 39); we will therefore call the original AD-Mpt5p isolate AD-Mpt5p[64–362].

To be certain that the Sst2p-Mpt5p interaction observed in the two-hybrid assays represented a true interaction, we constructed tagged proteins for biochemical analysis. Sst2p with an N-terminal HA1 epitope tag was expressed from the *PGK* promoter. YEp plasmids that contained the intact *MPT5* gene (39) were isolated, and a fusion of GST to intact Mpt5p (GST-Mpt5p) was constructed; GST-Mpt5p and the GST control were expressed from the *GAL1* promoter. The HA1-Sst2p and GST-Mpt5p constructs complemented *sst2* and *mpt5* mutations, respectively (data not shown). HA1-Sst2p copurified

TABLE 2. Two-hybrid screen

AD construct[a]	β-Galactosidase activity with BD construct[b]:					No. isolated from library[c]	
	SST2	*SNF1*	Lamin	p53	*CDK2*	cDNA	Genomic
MPT5	++++	−	−	−	−	1	0
ORF1	+++	+++	−	−	+++	4	0
ORF2	++++	++++	−	−	−	2	0
RIF1	++++	+	−	−	++	1	3
CDC23	++++	−	−	−	++	1	0
TyA	++++	++	−	−	+++	1	0
Vector	−	−	NT	NT	NT	NR	NR
SNF4	−	++++	NT	NT	NT	NR	NR

[a] Fusions to the Gal4p AD were in pACT. The *MPT5* construct isolated in the screen (AD-Mpt5p[64–362]) contains an internal portion of the gene.
[b] BD fusions were in pAS2, which contains the Gal4p BD and the HA1 epitope. β-Galactosidase activities were determined by the colony lift method. +, blue (the number of plus signs indicates the intensity); −, white; NT, not tested.
[c] AD constructs that could interact with BD-Sst2p were isolated from cDNA or genomic libraries. NR, not relevant.

with GST-Mpt5p in either the presence or absence of α-factor, whereas it did not copurify with GST (Fig. 1), indicating either that there is a direct interaction between Sst2p and Mpt5p or that the two proteins are present in the same complex.

MPT5 probes were used to analyze RNA expression by Northern analysis. A faint band of about 2.6 kb was detected (data not shown), consistent with the predicted size of the *MPT5* open reading frame (834 amino acids [39]). This RNA was present at similar levels in **a** and α cells, in either the presence or absence of pheromone, and in **a**/α cells.

Phenotypes of *mpt5* mutants. *MPT5* was previously identified by complementation of a mutant with a temperature-sensitive growth defect, but *mpt5* gene disruptions were observed to result in a slight increase in sensitivity to pheromone and a defect in recovery from pheromone arrest (39). These effects on pheromone response and recovery suggested that the interaction of Mpt5p with Sst2p was functionally important. To confirm the previously observed *mpt5* phenotypes, several disruptions and deletions were constructed. All of the disruptions and deletions resulted in the same set of phenotypes, which were similar to the phenotypes observed previously (39). The *mpt5* mutations resulted in temperature-sensitive growth in **a**/α diploids homozygous for an *mpt5* disruption (data not shown) as well as in haploids (Fig. 2).

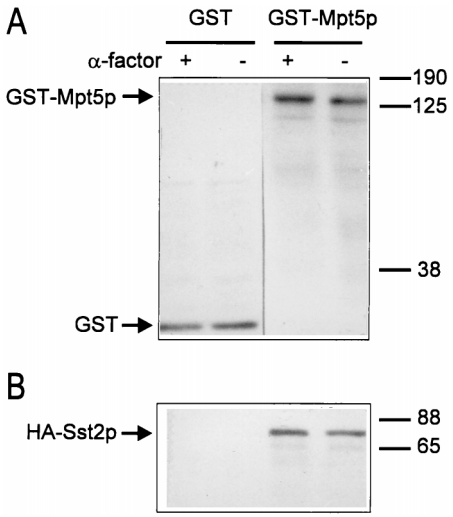

FIG. 1. Copurification of HA1-Sst2p with GST-Mpt5p. Wild-type (W303-1A) cells containing YEp*PGK-HA-SST2* and either p*GAL-GST* or p*GAL-GST-MPT5* were grown in selective medium containing raffinose and shifted to galactose medium for 4 h to induce the expression of GST or GST-Mpt5p, and half of the cells were treated with 100 nM α-factor for 1 h. GST-Mpt5p or GST was affinity purified from yeast extracts, run on an SDS-polyacrylamide gel, and immunoblotted with either anti-GST antibody (A) or anti-HA antibody 12CA5 (B). The results were reproduced in three independent experiments.

The effects of the *mpt5* and *sst2* mutations on pheromone response and recovery were compared. The **a** *mpt5* mutants were about fourfold more sensitive to α-factor than was the wild type in plate pheromone-spotting assays of growth arrest and assays of induction of a pheromone-inducible reporter construct (Fig. 3). This increase in pheromone sensitivity is considerably milder than the 200-fold increase in sensitivity of the *sst2* mutant (Fig. 3) (8). In the pheromone-spotting assay, the zone of growth arrest of wild-type strains was initially clear; however, with additional incubation, cells from the edges of the zone began to grow and the zone of growth arrest became turbid (Fig. 3A). The *sst2* mutant showed a larger zone of growth arrest that remained clear due to the defect in recovery from pheromone arrest (21). The zone of growth arrest of the *mpt5* mutants remained mostly clear (Fig. 3A), consistent with a defect in recovery, although the phenotype is more subtle than observed with *sst2* mutants. The *mpt5* mutations did not affect mating (Fig. 4B) and had similar effects in **a** and α strains (data not shown). An *sst2::HIS3 mpt5::URA3* (TCK19) double mutant showed the temperature-sensitive growth defect (Fig. 2) and the same pheromone response phenotype in halo assays as the *sst2* mutant (Fig. 3A), indicating that there was no synergistic effect between the two mutations.

Overexpression of *SST2* or *MPT5* increases recovery from pheromone arrest. In wild-type cells, expression of *SST2* under the control of the *PGK* promoter, which provides high-level, constitutive expression, resulted in halos that quickly became turbid (Fig. 5), suggesting that overexpression of Sst2p increases recovery from pheromone arrest. An *mpt5::HIS3* mutation reduced the promotion of recovery by YEp*PGK-SST2*, indicating that the effect of overexpression of Sst2p is partially dependent on the function of Mpt5p. The effect of a *kss1* mutation was also tested due to the suggested role of Kss1p in desensitization (16) and evidence that Kss1p can interact with Mpt5p (described below). The *kss1* mutation did not affect the phenotype resulting from YEp*PGK-SST2* (Fig. 5).

The *MPT5* putative open reading frame contains potential ATG initiation codons at positions 1 and 29 (39), making the site of initiation uncertain. Constructs that should express either the 834- or 806-amino-acid protein from the *PGK* pro-

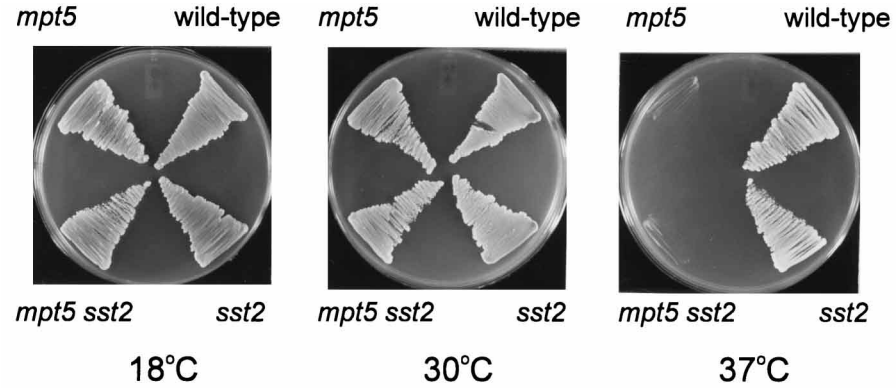

FIG. 2. *mpt5* growth defect. Wild-type (W303-1A), *mpt5::URA3* (TCK14), *sst2::HIS3* (RAK40), and *sst2::HIS3 mpt5::URA3* (TCK19) strains were streaked on YEPD medium and grown at 18, 30, or 37°C.

moter were made (*PGK-MPT5[1–834]* and *PGK-MPT5[29–834]*, respectively). Transformation of a wild-type strain with YEp*PGK-MPT5[1–834]* resulted in poor growth of transformants; small colonies were observed only after a long incubation period (Table 3). Unlike the temperature-sensitive *mpt5* growth defect, this transformation defect was observed at all temperatures. Transformation with YEp*PGK-MPT5[29–834]* gave rise to colonies of normal size with the same timing as the control vector. The *PGK-MPT5[29–834]* construct was unable to complement the temperature-sensitive growth or pheromone response defects of an *mpt5::URA3* mutant, suggesting that *MPT5[29–834]* was not functional. The transformation defect complicated assays of YEp*PGK-MPT5[1–834]* function; however, the growth of wild-type strains and of *mpt5::URA3* transformants containing YEp*PGK-MPT5[1–834]* at the restrictive temperature were similar, suggesting that *PGK-MPT5[1–834]* complements the temperature-sensitive growth defect of the *mpt5::URA3* mutation (Table 3). These results

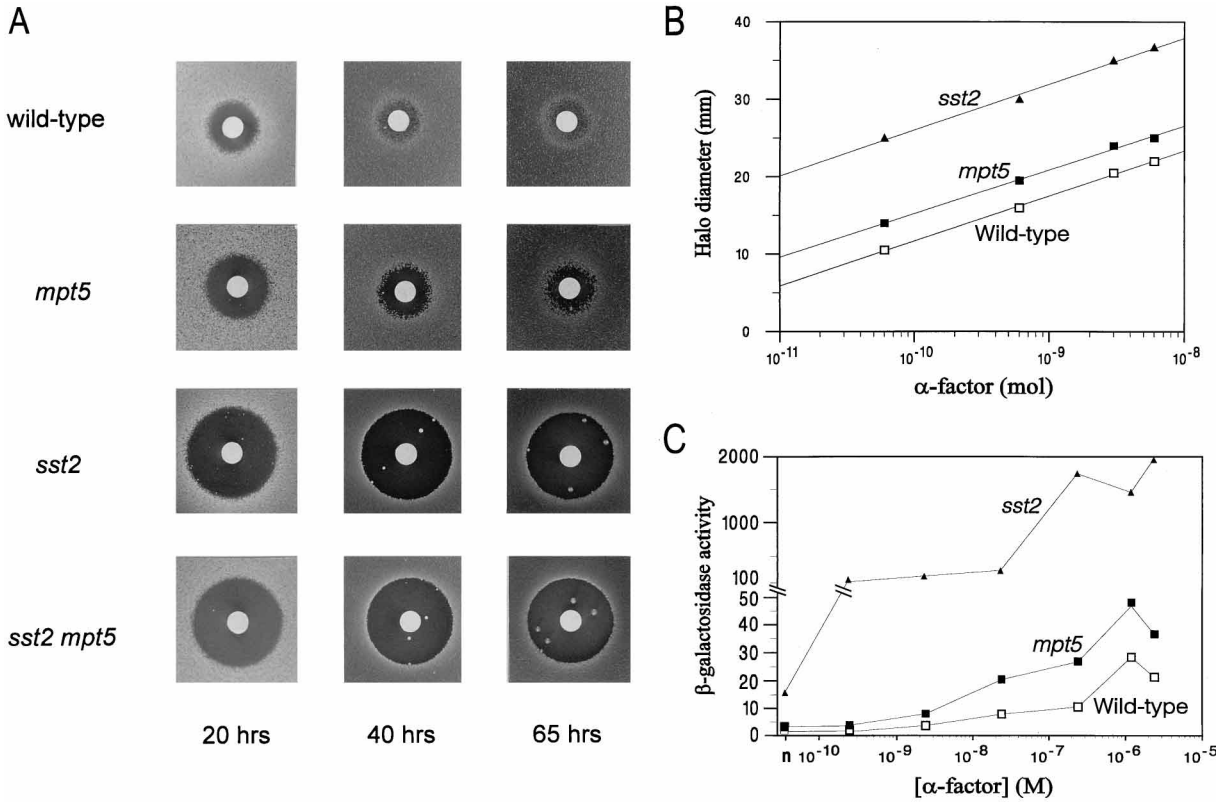

FIG. 3. Pheromone response and recovery assays. Wild-type (W303-1A), *mpt5::URA3* (TCK14), *sst2::HIS2* (RAK40), and *sst2::HIS3 mpt5::URA3* (TCK19) strains were tested for their response to pheromone. (A) Halo assays. A 5-μg aliquot of α-factor on filter disks was applied to nascent lawns of cells, which were incubated at 30°C for the times indicated. (B) Quantitation of halo diameters. Filters containing various amounts of α-factor were applied to lawns, and the diameters of the zones of growth inhibition were measured at 30 h; the data are averages of three independent assays. (C) Reporter gene activation assays. Cells containing a p*FUS1-lacZ* plasmid (pTCFL1) were induced with various concentrations of α-factor for 2 h at 30°C, and β-galactosidase activities were determined. The data are averages of three independent transformations, and differences between strains were statistically significant. n, no α-factor.

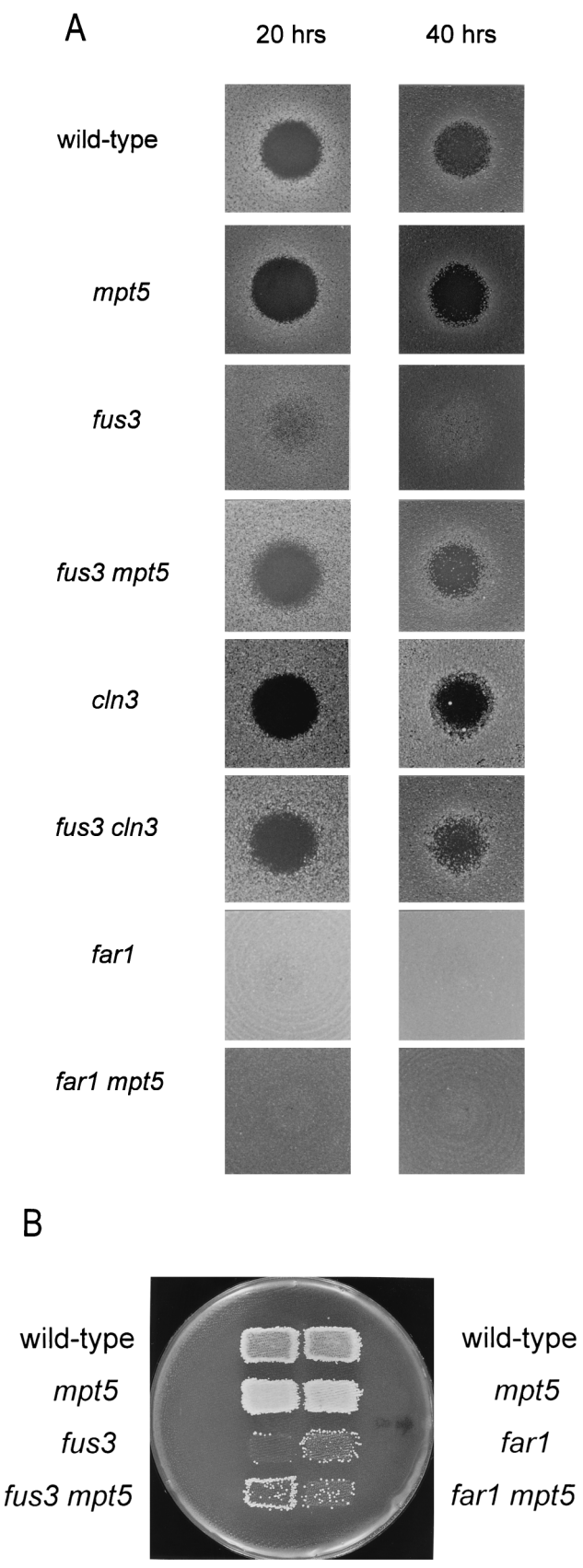

suggest that Mpt5p[1–834] is the intact, functional protein and that overexpression of Mpt5p is detrimental.

This inhibition of growth prevented the use of *PGK-MPT5* to test the effect of overexpression of Mpt5p on recovery from pheromone arrest, necessitating the use of a multicopy plasmid containing *MPT5* expressed from its own promoter for these assays. The wild-type strain containing YEp-*MPT5* showed a turbid zone of growth arrest (Fig. 5), suggesting that Mpt5p promotes recovery from pheromone arrest. YEp-*MPT5* did not increase recovery in an *sst2::HIS3* mutant (Fig. 5), indicating that Sst2p is essential for this effect. A *kss1::URA3* mutation had little or no effect, suggesting that Kss1p is not required for this effect.

Overexpression of Kss1p has previously been shown to result in a turbid halo in *sst2* and wild-type strains, suggesting a role for Kss1p in recovery (16). This effect was greatly reduced in the *mpt5::HIS3* mutant (Fig. 5), indicating that the ability of Kss1p overexpression to promote recovery depends partially on Mpt5p function but not on Sst2p function.

Mpt5p interacts with Fus3p and Kss1p. To determine whether Sst2p or Mpt5p interacts with known components of the pheromone response pathway, AD-Sst2p and a fusion containing intact Mpt5p (AD-Mpt5p[1–834]) were tested for interactions with BD fusions to Gpa1p, Ste20p, Ste21p, Ste5p, Ste11p, Ste7p, Fus3p, and Kss1p. No interactions were detected between AD-Sst2p and any of the BD constructs (data not shown). AD-Mpt5p showed interactions with BD-Fus3p and BD-Kss1p (Fig. 6) but not with the other BD-fusion proteins tested (data not shown). To determine whether this two-hybrid result represented a true interaction, the Mpt5p-Fus3p interaction was tested biochemically. Immunoprecipitation of Mpt5p with a C-terminal epitope tag (FLAG) resulted in coimmunoprecipitation of endogenous Fus3p, whereas Fus3p did not coimmunoprecipitate with a control FLAG construct (Fig. 7). The Mpt5p-Fus3p interaction was not affected by pheromone induction.

To investigate the functional relationship between Fus3p/Kss1p and Mpt5p, double mutants were constructed. A *kss1* single mutation does not result in changes in pheromone response or mating (16). The phenotype of the *kss1 mpt5* double mutant was similar to that of the *mpt5* single mutant in assays of temperature-sensitive growth, pheromone response, and mating; therefore, no synergistic effects of the two mutations were observed (data not shown).

fus3 null mutations result in decreased mating and response to pheromone and a defect in G_1 arrest in response to pheromone (Fig. 4) (28, 29). The *fus3 mpt5* double mutant showed the *mpt5* temperature-sensitive growth defect (data not shown). Surprisingly, the *mpt5* mutation restored pheromone-induced arrest to the *fus3::LEU2* null mutant (Fig. 4A); recovery of the *fus3 mpt5* double mutant from pheromone arrest was intermediate between those of the wild-type and *mpt5* strains. The *mpt5* null mutation also partially suppressed the mating defect of the *fus3* strain (Fig. 4B). Suppression of the *fus3* pheromone response defect by *mpt5* was similar to the suppression previously shown for a *cln3* mutation (Fig. 4A) (29). Also, the *cln3* single mutant showed an increase in size of the zone of growth arrest by pheromone similar to that of the *mpt5* mutant.

FIG. 4. Epistasis tests of *mpt5 fus3* and *mpt5 far1* double mutants. Wild-type (W303-1A), *mpt5::HIS3* (TCK13), *fus3::LEU2* (RAK29), *mpt5::HIS3 fus3::LEU2* (TCK24), *cln3::URA3* (TCK31), *cln3::URA3 fus3::LEU2* (TCK28), *far1::ADE2* (TCK21), and *far1::ADE2 mpt5::HIS3* (TCK25) strains were tested for pheromone response by halo assays (A) and for mating (B).

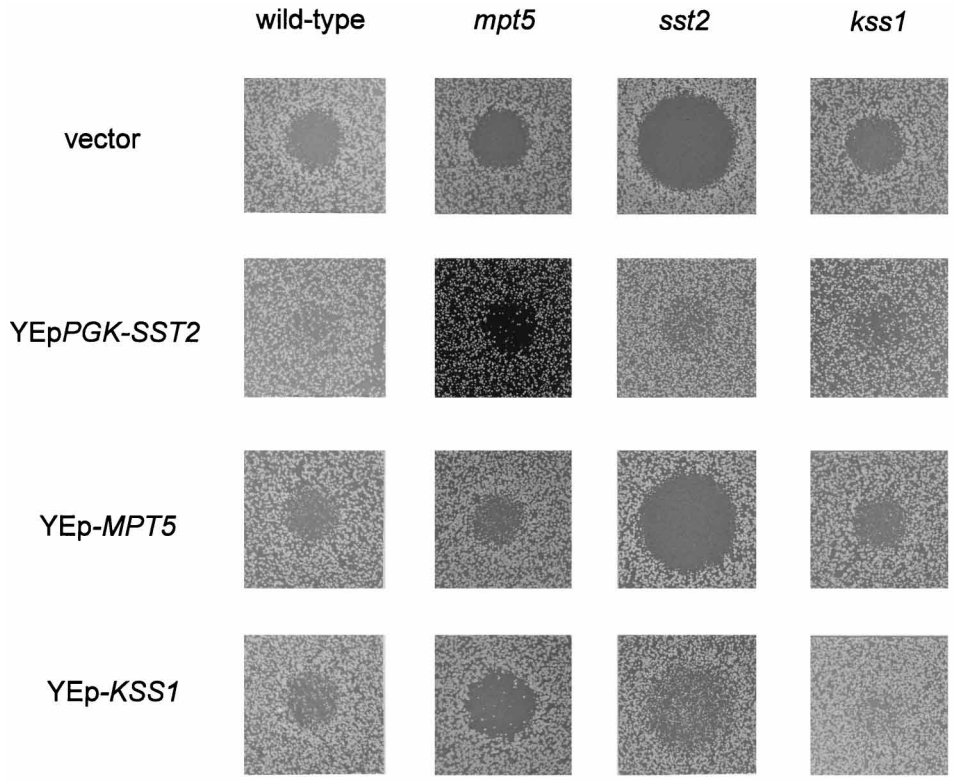

FIG. 5. Overexpression of Mpt5p, Sst2p, and Kss1p. Wild-type (W303-1A), *sst2::HIS3* (RAK40), *mpt5::HIS3* (TCK13), and *kss1::HIS3* (TCK9) strains containing either the YEp vector (pRS425), YEp-*MPT5* (pRS425-*MPT5*), p*PGK-SST2*, or YEp-*KSS1* (pXT1) were spread on plates, 5 μg of α-factor was spotted on the nascent lawns, and the plates were incubated at 30°C for 40 h.

Because the role of Fus3p in G_1 arrest acts through phosphorylation of Far1p (32, 55, 67), the functional relationship between Mpt5p and Far1p was also investigated. A *far1::ADE2 mpt5::HIS3* double mutant showed the *mpt5* temperature-sensitive growth defect (data not shown) and did not suppress the *far1* pheromone arrest or mating defects (Fig. 4).

Mpt5p interacts with Cdc28p. The ability of either an *mpt5* or a *cln3* mutation to suppress the *fus3* defect in pheromone-induced arrest (Fig. 4A) (17, 28, 29) was intriguing because G_1 arrest by pheromone occurs through inhibition of G_1 cyclin-Cdc28p activity (56, 67). We therefore tested interactions of Mpt5p with the G_1 cyclins or Cdc28p kinase by using the two-hybrid system. No interaction was detected between AD-Mpt5p and BD fusions to Cln1p, Cln2p, or Cln3p, although BD-Cln2p and BD-Cln3p showed high basal activation, which could mask an interaction (data not shown). Interestingly, an interaction between AD-Mpt5p and BD-Cdc28p was observed in both wild-type and *far1* strains (Fig. 6). This interaction was confirmed by coimmunoprecipitation of endogenous Cdc28p with Mpt5p-FLAG (Fig. 7). The Mpt5p-Cdc28p interaction was not affected by pheromone induction.

TABLE 3. Activities of Mpt5p constructs

MPT5 construct[a]	Plasmid	Growth of transformants[b]	Complementation of *mpt5*[c]	
			Halo[d]	37°C growth[e]
None	Vector	+++	−	−
Mpt5p[1–834]	YCp	+++	+++	+++
	YEp*PGK*	+	NT	+
Mpt5p[29–834]	YEp*PGK*	+++	−	−

[a] *MPT5* was expressed either under its own promoter (YCp) or under the *PGK* promoter (YEp*PGK*).
[b] The plasmids were transformed into the wild-type strain (W303-1A). +++, wild-type growth; +, colonies that were first visible 1 day after the wild type and remained small.
[c] The plasmids were transformed into the *mpt5::URA3* mutant (TCK14).
[d] +++, wild-type phenotype; −, *mpt5* phenotype; NT, not tested.
[e] +++, wild-type growth at 37°C; +, reduced growth; −, *mpt5* phenotype.

Characterization of Sst2p- and Fus3p/Kss1p-interacting domains of Mpt5p. To delineate regions of Mpt5p involved in the interactions with Sst2p, Fus3p, Kss1p, and Cdc28p, deletion derivatives of AD-Mpt5p were tested (Fig. 6). The original Mpt5p[64–362] construct identified the smallest fragment sufficient for the interaction with BD-Sst2p, although the interaction with intact Mpt5p[1–834] was severalfold stronger. Removal of the N-terminal 28 amino acids, which were shown to be necessary for Mpt5p function, as described above, increased the strength of the Sst2p-Mpt5p interaction about 10-fold. Removal of amino acids 29 to 66 (Mpt5p[67–834]) reduced activity, indicating that this region contributes to the interaction. Removal of C-terminal sequences (compare Mpt5p[64–362] and Mpt5p[67–834]) had no significant effect. Thus, the Sst2p interaction domain is between amino acids 67 and 362 of Mpt5p, with sequences between amino acids 29 and 66 facilitating the interaction and amino acids 1 to 28 inhibiting the interaction.

The similar patterns of interaction observed for BD-Fus3p and BD-Kss1p suggest that these two MAP kinase homologs (28) interact with the same region of Mpt5p (Fig. 6). The

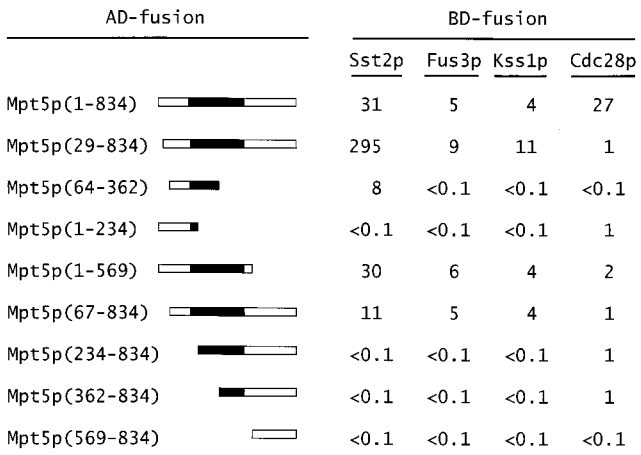

AD-fusion	BD-fusion			
	Sst2p	Fus3p	Kss1p	Cdc28p
Mpt5p(1-834)	31	5	4	27
Mpt5p(29-834)	295	9	11	1
Mpt5p(64-362)	8	<0.1	<0.1	<0.1
Mpt5p(1-234)	<0.1	<0.1	<0.1	1
Mpt5p(1-569)	30	6	4	2
Mpt5p(67-834)	11	5	4	1
Mpt5p(234-834)	<0.1	<0.1	<0.1	1
Mpt5p(362-834)	<0.1	<0.1	<0.1	1
Mpt5p(569-834)	<0.1	<0.1	<0.1	<0.1

FIG. 6. Analysis of Mpt5p binding regions. Various AD-Mpt5p fusion constructs, with the region containing the conserved eight tandem repeats (15) shown in black, were tested for interactions with BD-Sst2p, BD-Fus3p, BD-Kss1p, and BD-Cdc28p fusions in the *far1::ADE2* mutant. β-Galactosidase units were averages of assays of at least three independent transformations; the standard deviations varied from <10 to 20% of the mean values. For comparison, the activity of AD-Snf4p with BD-Snf1p was 7 U in these assays. BD-Kss1p had a low basal induction of β-galactosidase activity (1.0 U), which has been subtracted from the activities for the interactions with the various AD-Mpt5p fusions; the other constructs had no detectable background.

N-terminal 66 amino acids and the C-terminal 266 amino acids of Mpt5p (constructs Mpt5p[67–834] and Mpt5p[1–569], respectively) were not essential for the interactions with Fus3p or Kss1p, whereas longer truncations did prevent these interactions. Therefore, Fus3p and Kss1p interact with the region of Mpt5p between residues 67 and 569. The N-terminal 28 amino acids may have a mild inhibitory effect on these interactions. Thus, the regions of Mpt5p involved in the interactions with Sst2p and Fus3p/Kss1p may overlap, although more detailed analysis is necessary to define the interacting domains precisely.

The assays of the various AD-Mpt5p constructs for interactions with BD-Cdc28p did not define a particular region involved in the interaction; both N- and C-terminal truncations greatly reduced the interaction (Fig. 6). However, it is interesting that the N-terminal 28 amino acids of Mpt5p, which inhibit the Sst2p interaction and possibly the Fus3p and Kss1p interactions, are essential for a strong interaction with BD-Cdc28p.

DISCUSSION

Mpt5p may play multiple roles. We identified Mpt5p by its ability to interact with Sst2p in the two-hybrid system, consistent with its playing roles in both pheromone sensitivity and desensitization to pheromone. *MPT5* has also been identified by complementation of a temperature-sensitive mutant (39) and as a multicopy suppressor of a *pop2* mutation (accession no. D26184), which results in a defect in derepression by glucose and a temperature-sensitive growth defect (61). *mpt5* mutations result in several phenotypes including a temperature-sensitive growth defect (Fig. 2), which has been shown to occur at the G_2/M phase of the cell cycle (39). The interaction of Mpt5p with Cdc28p (Fig. 6) may play a role in the arrest at G_2/M as well as the proposed role in pheromone sensitivity and recovery discussed below.

Consistent with our discovery of an interaction between Sst2p and Mpt5p, previous analysis of *mpt5* disruption mutations had indicated an increase in pheromone sensitivity and recovery from G_1 arrest by pheromone (39). Both of these effects are much milder in *mpt5* mutants than in *sst2* mutants (Fig. 3). However, the promotion of recovery by overexpression of either Sst2p under *PGK* control or Mpt5p on a high-copy plasmid (Fig. 5) provides additional evidence for a role of Mpt5p as well as Sst2p in recovery.

Very high level expression of Mpt5p under *PGK* control was detrimental to growth (Table 3). Whether this phenotype is related to the other phenotypes associated with *mpt5* is unclear.

Mpt5p is a member of a family of proteins from yeast, *Drosophila*, and humans that contain a conserved motif of eight tandem repeats (15). Most members of this tandem repeat family, including the yeast gene *YGL023* (9), were identified in genome-sequencing projects, and their functions are unknown. The only member of this tandem repeat family for which functional information is available is the *Drosophila Pumilio* gene, which is involved in formation of abdominal segments during early embryogenesis and is implicated in translational regulation (3, 46, 52).

What is the role of Mpt5p in pheromone sensitivity and recovery? The ability of Mpt5p to interact with the MAP kinase homologs Fus3p and Kss1p (Fig. 6 and 7) could indicate either that the MAP kinases are targets for Mpt5p or that Mpt5p is a MAP kinase substrate. Mutation of a perfect MAP kinase consensus sequence (14, 54) in the *MPT5* N terminus did not affect the temperature sensitivity or pheromone response phenotypes (data not shown).

The mild increase in the sensitivity to pheromone of *mpt5* mutants is similar to the phenotype resulting from overexpression of Fus3p (29) or dominant gain-of-function *FUS3* mutants (6), suggesting that Fus3p and Mpt5p may have opposite functions. Interestingly, *fus3* mutants show reduced pheromone-induced arrest and mating, and either an *mpt5* or a *cln3* mutation can partially suppress the pheromone arrest (Fig. 4A) (28, 29) and mating (Fig. 4B) (data not shown) defects. Also, both the *mpt5* and *cln3* mutants showed a mild increase in pheromone sensitivity in the pheromone-spotting assay. There-

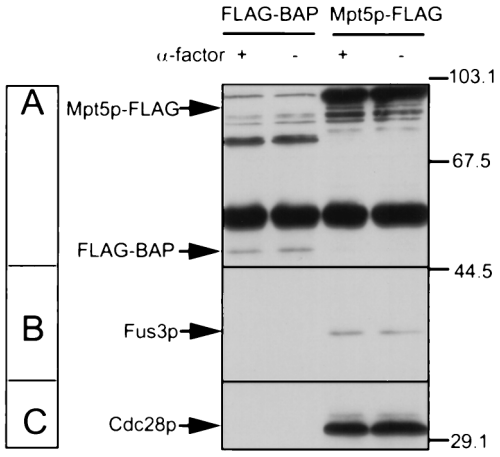

FIG. 7. Coimmunoprecipitation of Mpt5p-FLAG with Fus3p and Cdc28p. Wild-type (W303-1A) cells containing either YEp-*MPT5-FLAG* or YEpFLAG-1 BAP were grown in selective medium, and half of the cells were treated with 100 nM α-factor for 1 h. Mpt5p-FLAG or FLAG-BAP was immunoprecipitated from yeast extracts with anti-FLAG M2 affinity gel, run on an SDS-polyacrylamide gel, and immunoblotted with either anti-FLAG antibody (A), anti-Fus3p antibody (B), or anti-Cdc28p antibody (C). The results were reproduced in at least three independent experiments.

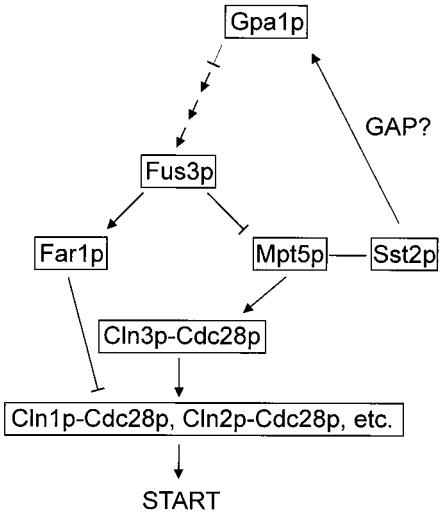

FIG. 8. Speculations on Mpt5p function. Standard arrows indicate a positive role, and blunt arrows indicate a negative role. Because either *cln3* or *mpt5* mutations suppress *fus3*, we show Mpt5p acting below Fus3p. Based on the interaction of Mpt5p with Cdc28p and the similar suppression and pheromone sensitivity phenotypes of *cln3* and *mpt5* mutants, we propose that Mpt5p acts through Cln3p-Cdc28p. Although Cln1p, Cln2p, and Cln3p were originally thought to have equivalent, functionally redundant roles (18, 59), numerous differences have led to a model in which the role of Cln3p is to positively regulate Cln1p, Cln2p, and possibly other G_1 cyclins (45, 68). The opposite phenotypes of *fus3* and *mpt5* suggest that they play opposite roles; in this diagram, we show Fus3p acting negatively on Mpt5p. An *sst2* mutation prevents the effect of overexpression of *MPT5*, indicating that Sst2p is necessary for promotion of recovery by Mpt5p. An *mpt5* mutation only partially reduces the effect of overexpression of *SST2*. We propose that this partial effect is due to two roles for Sst2p; one role would act through Mpt5p, and the second role would act on the Gα subunit Gpa1p, based on the identification of a family of Sst2p homologs that act as GAPs for Gα subunits.

fore, we suggest that both Mpt5p and Cln3p act downstream of Fus3p and that Mpt5p acts in the same pathway as Cln3p (Fig. 8). Kikuchi et al. (39) showed that an *mpt5* mutation does not affect the pheromone resistance resulting from the *CLN3-2* dominant mutation (17), consistent with Cln3p acting downstream of Mpt5p.

Based on the similar effects of *mpt5* and *cln3* mutations in a *fus3* mutant, we tested the ability of Mpt5p to interact with the G_1 cyclins and Cdc28p. Based on the ability of Mpt5p to interact with Cdc28p (Fig. 6 and 7), we speculate that the role of Mpt5p is to activate Cln3p-Cdc28p, which in turn would increase Cln1p-Cdc28p and Cln2p-Cdc28p activity (Fig. 8). In an *mpt5* mutant, Cln3p-Cdc28p activity would be reduced, resulting in lower Cln1p-Cdc28p and Cln2p-Cdc28p activity and allowing cell cycle arrest at lower pheromone concentrations. The role of Mpt5p in recovery could also act through Cln3p-Cdc28p.

Because Far1p plays an important role in cell cycle arrest by the inhibition of Cln1p-Cdc28p and Cln2p-Cdc28p (56), we also considered the possibility that Mpt5p could promote recovery through Far1p. We have not detected an interaction between Far1p and Mpt5p in the two-hybrid system, although this assay was complicated by the ability of fusions of the Gal4p BD to either Far1p or Mpt5p to activate reporter gene expression. Unlike the results with the *fus3* mutant, *mpt5* mutations did not restore G_1 arrest to a *far1* mutant (Fig. 4A), which is consistent with a role for Mpt5p through either Far1p or Cln3p-Cdc28p. Far1p is not required for the interaction between Mpt5p and Cdc28p in the two-hybrid system, indicating that Far1p is not acting as a bridging protein. The complexity of regulation of the components that act in transit through the G_1 phase of the cell cycle and in cell cycle arrest during pheromone response means that many mechanisms for Mpt5p action are possible. However, the model shown in Fig. 8 fits the protein-protein and genetic interactions observed and provides a working hypothesis useful in approaching the analysis of the role of Mpt5p.

Is Sst2p a bifunctional protein? Recent results with yeast have suggested that Sst2p acts at the level of the Gα subunit Gpa1p (22, 23). In addition, a family of Sst2p homologs (called RGS proteins) that act as GTPase-activating proteins (GAPs) for Gα subunits has been identified (24, 37). The position of Sst2p action in our model (Fig. 8) does not fit these other results. We did not detect an interaction between Sst2p and Gpa1p in the two-hybrid system (data not shown), although a two-hybrid interaction between $G\alpha_{i3}$ and the mammalian Sst2p homolog GAIP was detected (19). However, GAIP has been shown to act as a GAP for $G\alpha_q$ (35), although an interaction between $G\alpha_q$ and the RGS protein GAIP was not been detected in the two-hybrid system (19), indicating that not all Gα-RGS interactions can be detected with this system.

We postulate that Sst2p has two functions in pheromone sensitivity and recovery. The RGS domain function would act on Gpa1p, and a separate function would act through Mpt5p (Fig. 8). Most of the RGS proteins are much smaller than Sst2p and consist mostly of the RGS domain. Unlike most RGS family members, *Aspergillus flbA*, which is involved in conidiophore development and sporulation, shows extensive sequence similarity to *SST2* throughout most of the coding region (43); both proteins contain a long N-terminal domain in addition to the C-terminal RGS domain. Interestingly, it has recently been proposed that flbA has more than one mechanism of action (71). The proposal that Sst2p has two functions, one through the RGS domain and a second through Mpt5p, is consistent with the observation that stimulation of recovery by Sst2p overexpression was only partially dependent on Mpt5p (Fig. 5). An *mpt5* mutation would affect only the Mpt5p-dependent effect of Sst2p overexpression but not the effect of RGS domain activity. The characterization of the RGS family as Gα GAPs has helped to elucidate the formerly elusive role of Sst2p. The further characterization of Mpt5p-dependent roles of Sst2p, as well as RGS function, and the characterization of flbA and other RGS family members for possible functions separate from the RGS GAP function should continue to provide interesting information on this important regulatory family.

ACKNOWLEDGMENTS

We thank S. Elledge and S. Fields for libraries and other two-hybrid system reagents; R. Akada for strains and plasmids; W. Courchesne, S. DeSimone, F. Cross, S. Seifert, J. Printen, and G. Sprague for plasmids; D. Pecchia for oligonucleotides, B. Futcher for antibodies; C. Staats for technical assistance; and H. de Nobel, L. Kallal, S. DeSimone, J. Pike, and B.-E Xu for comments on the manuscript.

This work was supported by National Institutes of Health grant GM40585.

REFERENCES

1. **Akada, R., L. Kallal, D. I. Johnson, and J. Kurjan.** 1996. Genetic relationships between the G protein βγ complex, Ste5p, Ste20p, and Cdc42p: investigation of effector roles in the yeast pheromone response pathway. Genetics **143:**103–117.
2. **Ausubel, F. M., R. Brent, R. E. Kingston, D. D. Moore, J. G. Seidman, J. A. Smith, and K. Struhl.** 1989. Current protocols in molecular biology, p. 13.6.1–13.6.4. John Wiley & Sons, Inc., New York, N.Y.
3. **Barker, D. D., C. Wang, J. Moore, L. K. Dickinson, and R. Lehman.** 1992. Pumilio is essential for function but not for distribution of the *Drosophila* abdominal determinant Nanos. Genes Dev. **6:**2312–2326.

4. **Bartel, P., C.-T. Chien, R. Sternglanz, and S. Fields.** 1993. Elimination of false positives that arise in using the two-hybrid system. BioTechniques **14:**920–924.
5. **Breeden, L., and K. Nasmyth.** 1985. Regulation of the yeast *HO* gene. Cold Spring Harbor Symp. Quant. Biol. **50:**643–650.
6. **Brill, J. A., E. A. Elion, and G. R. Fink.** 1994. A role for autophosphorylation revealed by activated alleles of *FUS3*, the yeast MAP kinase homolog. Mol. Biol. Cell **5:**297–312.
7. **Chan, R. K., and C. A. Otte.** 1982. Isolation and genetic analysis of *Saccharomyces cerevisiae* mutants supersensitive to G1 arrest by **a** factor and α factor pheromones. Mol. Cell. Biol. **2:**11–20.
8. **Chan, R. K., and C. A. Otte.** 1982. Physiological characterization of *Saccharomyces cerevisiae* mutants supersensitive to G1 arrest by **a** factor and α factor pheromones. Mol. Cell. Biol. **2:**21–29.
9. **Chen, W., E. Balzi, E. Capieaux, and A. Goffeau.** 1991. The YGL023 gene encodes a putative regulatory protein. Yeast **7:**309–312.
10. **Chien, C.-T., P. L. Bartel, R. Sternglanz, and S. Fields.** 1991. The two-hybrid system: a method to identify and clone genes for proteins that interact with a protein of interest. Proc. Natl. Acad. Sci. USA **88:**9578–9582.
11. **Choi, K.-Y., B. Satterberg, D. M. Lyons, and E. A. Elion.** 1994. Ste5 tethers multiple protein kinases in the MAP kinase cascade required for mating in S. cerevisiae. Cell **78:**499–512.
12. **Christianson, T. W., R. S. Sikorski, M. Dante, J. H. Shero, and P. Hieter.** 1992. Multifunctional yeast high-copy-number shuttle vectors. Gene **110:** 119–122.
13. **Clare, J., and P. Farabaugh.** 1985. Nucleotide sequence of a yeast Ty element: evidence for an unusual mechanism of gene expression. Proc. Natl. Acad. Sci. USA **82:**2829–2833.
14. **Clark-Lewis, I., J. S. Sanghera, and S. L. Pelech.** 1991. Definition of a consensus sequence for peptide substrate recognition by $p44^{mpk}$, the meiosis-activated myelin basic protein kinase. J. Biol. Chem. **266:**15180–15184.
15. **Coglievina, M., I. Bertani, R. Klima, P. Zaccaria, and C. V. Bruschi.** 1995. The DNA sequence of a 7941 bp fragment of the left arm of chromosome VII of *Saccharomyces cerevisiae* contains four open reading frames including the multicopy suppressor of the *pop2* mutation and a putative serine/threonine protein kinase gene. Yeast **11:**767–774.
16. **Courchesne, W. E., R. Kunisawa, and J. Thorner.** 1989. A putative protein kinase overcomes pheromone-induced arrest of cell cycling in *S. cerevisiae*. Cell **58:**1107–1119.
17. **Cross, F.** 1988. *DAF1*, a mutant gene affecting size control, pheromone arrest, and cell cycle kinetics of *Saccharomyces cerevisiae*. Mol. Cell. Biol. **8:**4675–4684.
18. **Cross, F. R.** 1990. Cell cycle arrest caused by *CLN* gene deficiency in *Saccharomyces cerevisiae* resembles START-I arrest and is independent of the mating-pheromone signalling pathway. Mol. Cell. Biol. **10:**6482–6490.
19. **De Vries, L., M. Mousli, A. Wurmser, and M. G. Farquhar.** 1995. GAIP, a protein that specifically interacts with the trimeric G protein $G\alpha_{i3}$, is a member of a protein family with a highly conserved core domain. Proc. Natl. Acad. Sci. USA **92:**11916–11920.
20. **Dietzel, C., and J. Kurjan.** 1987. The yeast *SCG1* gene: a Gα-like protein implicated in the **a**- and α-factor response pathway. Cell **50:**1001–1010.
21. **Dietzel, C., and J. Kurjan.** 1987. Pheromonal regulation and sequence of the *Saccharomyces cerevisiae SST2* gene: a model for desensitization to pheromone. Mol. Cell. Biol. **7:**4169–4177.
22. **Dohlman, H. G., D. Apaniesk, Y. Chen, J. Song, and D. Nusskern.** 1995. Inhibition of G-protein signaling by dominant gain-of-function mutations in Sst2p, a pheromone desensitization factor in *Saccharomyces cerevisiae*. Mol. Cell. Biol. **15:**3635–3643.
23. **Dohlman, H. G., J. Song, D. Ma, W. E. Courchesne, and J. Thorner.** 1996. Sst2, a negative regulator of pheromone signaling in the yeast *Saccharomyces cerevisiae*: expression, localization, and genetic interaction and physical association with Gpa1 (the G-protein α subunit). Mol. Cell. Biol. **16:**5194–5209.
24. **Dohlman, H. G., and J. Thorner.** 1997. RGS proteins and signaling by heterotrimeric G proteins. J. Biol. Chem. **272:**3871–3874.
25. **Doi, A., and K. Doi.** 1990. Cloning and nucleotide sequence of the *CDC23* gene of *Saccharomyces cerevisiae*. Gene **91:**123–126.
26. **Dolan, J. W., C. Kirkman, and S. Fields.** 1989. The yeast STE12 protein binds to the DNA sequence mediating pheromone induction. Proc. Natl. Acad. Sci. USA **86:**5703–5707.
27. **Ecker, D. J., M. I. Khan, J. Marsh, T. R. Butt, and S. T. Crooke.** 1987. Chemical synthesis and expression of a cassette adapted ubiquitin gene. J. Biol. Chem. **262:**3524–3527.
28. **Elion, E. A., J. A. Brill, and G. R. Fink.** 1991. FUS3 represses CLN1 and CLN2 and in concert with KSS1 promotes signal transduction. Proc. Natl. Acad. Sci. USA **88:**9392–9396.
29. **Elion, E. A., P. L. Grisafi, and G. R. Fink.** 1990. FUS3 encodes a cdc2+/CDC28-related kinase required for the transition from mitosis into conjugation. Cell **60:**649–664.
30. **Elion, E. A., B. Satterberg, and J. E. Kranz.** 1993. FUS3 phosphorylates multiple components of the mating signal transduction cascade: evidence for STE12 and FAR1. Mol. Biol. Cell **4:**495–510.
31. **Errede, B., and G. Ammerer.** 1989. STE12, a protein involved in cell-type-specific transcription and signal transduction in yeast, is part of protein-DNA complexes. Genes Dev. **3:**1349–1361.
32. **Errede, B., A. Gartner, Z. Zhou, K. Nasmyth, and G. Ammerer.** 1993. MAP kinase-related FUS3 from *S. cerevisiae* is activated by STE7 *in vitro*. Nature **362:**261–264.
33. **Hardy, C. F., L. Sussel, and D. Shore.** 1992. A RAP1-interacting protein involved in transcriptional silencing and telomere length regulation. Genes Dev. **6:**801–814.
34. **Harper, J. W., G. R. Adami, N. Wei, K. Keyomarsi, and S. J. Elledge.** 1993. The p21 Cdk-interacting protein Cip1 is a potent inhibitor of G1 cyclin-dependent kinases. Cell **75:**805–816.
35. **Hepler, J. R., D. M. Berman, A. G. Gilman, and T. Kozasa.** 1997. RGS4 and GAIP are GTPase-activating proteins for $G_{q\alpha}$ and block activation of phospholipase Cβ by γ-thio-GTP-$G_{q\alpha}$. Proc. Natl. Acad. Sci. USA **94:**428–432.
36. **Herskowitz, I., and R. E. Jensen.** 1994. Putting the HO gene to work: practical uses for mating-type switching. Methods Enzymol. **194:**132–146.
37. **Iyengar, R.** 1997. There are GAPS and there are GAPS. Science **275:**42–43.
38. **Kang, Y.-S., J. Kane, J. Kurjan, J. M. Stadel, and D. J. Tipper.** 1990. Effects of expression of mammalian Gα and hybrid mammalian-yeast Gα proteins on the yeast pheromone response signal transduction pathway. Mol. Cell. Biol. **10:**2582–2590.
39. **Kikuchi, Y., Y. Oka, M. Kobayashi, Y. Uesono, A. Toh-E, and A. Kikuchi.** 1994. A new yeast gene, *HTR1*, required for growth at high temperature, is needed for recovery from mating pheromone-induced G1 arrest. Mol. Gen. Genet. **245:**107–116.
40. **Kranz, J. E., B. Satterberg, and E. A. Elion.** 1994. The MAP kinase Fus3 associates with and phosphorylates the upstream signaling component Ste5. Genes Dev. **8:**313–327.
41. **Kurjan, J.** 1993. The pheromone response pathway in *Saccharomyces cerevisiae*. Annu. Rev. Genet. **27:**147–179.
42. **Leberer, E., D. Dignard, D. Harcus, D. Y. Thomas, and M. Whiteway.** 1992. The protein kinase homologue Ste20p is required to link the yeast pheromone response G-protein βγ subunits to downstream signalling components. EMBO J. **11:**4815–4824.
43. **Lee, B. N., and T. H. Adams.** 1994. Overexpression of *flbA*, an early regulator of *Aspergillus* asexual sporulation, leads to activation of *brlA* and premature initiation of development. Mol. Microbiol. **14:**323–324.
44. **Levin, D. E., and B. Errede.** 1995. The proliferation of MAP kinase signaling pathways in yeast. Curr. Opin. Cell Biol. **7:**197–202.
45. **Levine, K., K. Huang, and F. R. Cross.** 1996. *Saccharomyces cerevisiae* G_1 cyclins differ in their intrinsic functional specificities. Mol. Cell. Biol. **16:** 6794–6803.
46. **Macdonald, P. M.** 1992. The *Drosophila pumilio* gene: an unusually long transcription unit and an unusual protein. Development **114:**221–232.
47. **Marcus, S., A. Polverino, M. Barr, and M. Wigler.** 1994. Complexes between STE5 and components of the pheromone-responsive mitogen-activated protein kinase module. Proc. Natl. Acad. Sci. USA **91:**7762–7766.
48. **Marsh, L., A. M. Neiman, and I. Herskowitz.** 1991. Signal transduction during pheromone response in yeast. Annu. Rev. Cell Biol. **7:**699–728.
49. **Mitchell, D. A., T. K. Marshall, and R. J. Deschenes.** 1993. Vectors for the inducible overexpression of glutathione S-transferase fusion proteins in yeast. Yeast **9:**715–723.
50. **Miyajima, I., M. Nakafuku, N. Nakayama, C. Brenner, A. Miyajima, K. Kaibuchi, K. Arai, Y. Kaziro, and K. Matsumoto.** 1987. GPA1, a haploid-specific essential gene, encodes a yeast homolog of mammalian G protein which may be involved in mating factor signal transduction. Cell **50:**1011–1019.
51. **Moore, S. A.** 1983. Comparison of dose-responsive curves for alpha factor-induced agglutinin, cell division arrest, and projection formation of *Saccharomyces cerevisiae MAT***a** yeast cells. J. Biol. Chem. **258:**13849–13856.
52. **Murata, Y., and R. P. Wharton.** 1995. Binding of pumilio to maternal *hunchback* mRNA is required for posterior patterning in Drosophila embryos. Cell **80:**747–756.
53. **Özcan, S., K. Freidel, A. Leuker, and M. Ciriacy.** 1993. Glucose uptake and catabolite repression in dominant *HTR1* mutants of *Saccharomyces cerevisiae*. J. Bacteriol. **175:**5520–5528.
54. **Pelech, S. L., and J. S. Sanghera.** 1992. Mitogen-activated protein kinases: versatile transducers for cell signaling. Trends Biochem. Sci. **17:**233–238.
55. **Peter, M., A. Gartner, J. Horecka, G. Ammerer, and I. Herskowitz.** 1993. FAR1 links the signal transduction pathway to the cell cycle machinery in yeast. Cell **73:**747–760.
56. **Peter, M., and I. Herskowitz.** 1994. Direct inhibition of the yeast cyclin-dependent kinase Cdc28-Cln by Far1. Science **265:**1228–1231.
57. **Printen, J. A., and G. F. Sprague, Jr.** 1994. Protein-protein interactions in the yeast pheromone response pathway: Ste5p interacts with all members of the MAP kinase cascade. Genetics **138:**609–619.
58. **Ramer, S. W., and R. W. Davis.** 1993. A dominant truncation allele identifies a gene, *STE20*, that encodes a putative protein kinase necessary for mating in *Saccharomyces cerevisiae*. Proc. Natl. Acad. Sci. USA **90:**452–456.
59. **Richardson, H. E., C. Wittenberg, F. Cross, and S. I. Reed.** 1989. An essential G1 function for cyclin-like proteins in yeast. Cell **59:**1127–1133.

60. **Rothstein, R. J.** 1983. One-step gene disruption in yeast. Methods Enzymol. **101:**202–211.
61. **Sakai, A., T. Chibazakura, Y. Shimizu, and F. Hishinuma.** 1992. Molecular analysis of *POP2* gene, a gene required for glucose-derepression of gene expression in *Saccharomyces cerevisiae*. Nucleic Acids Res. **20:**6227–6233.
62. **Schreuder, M. P., S. Brekelmans, H. van den Ende, and F. M. Klis.** 1993. Targeting of a heterologous protein to the cell wall of *Saccharomyces cerevisiae*. Yeast **9:**399–409.
63. **Seifert, H. S., E. Y. Chen, M. So, and F. Heffron.** 1986. Shuttle mutagenesis: a method of transposon mutagenesis for *Saccharomyces cerevisiae*. Proc. Natl. Acad. Sci. USA **83:**737–739.
64. **Sikorski, R. S., and P. Hieter.** 1989. A system of shuttle vectors and yeast host strains designed for efficient manipulation of DNA in *Saccharomyces cerevisiae*. Genetics **122:**19–27.
65. **Song, O.-K., J. W. Dolan, Y.-L. O. Yuan, and S. Fields.** 1991. Pheromone-dependent phosphorylation of the yeast STE12 protein correlates with transcriptional activation. Genes Dev. **5:**741–750.
66. **Trueheart, J., J. D. Boeke, and G. R. Fink.** 1987. Two genes required for cell fusion during yeast conjugation: evidence for a pheromone-induced surface protein. Mol. Cell. Biol. **7:**2316–2328.
67. **Tyers, M., and B. Futcher.** 1993. Far1 and Fus3 link the mating pheromone signal transduction pathway to three G_1-phase Cdc28 kinase complexes. Mol. Cell. Biol. **13:**5659–5669.
68. **Tyers, M., G. Tokiwa, and B. Futcher.** 1993. Comparison of the Saccharomyces cerevisiae G1 cyclins: Cln3 may be an upstream activator of Cln1, Cln2, and other cyclins. EMBO J. **12:**1955–1968.
69. **Tyers, M., G. Tokiwa, R. Nash, and B. Futcher.** 1992. The Cln3-Cdc28 kinase complex of *S. cerevisiae* is regulated by proteolysis and phosphorylation. EMBO J. **11:**1773–1784.
70. **Whiteway, M., L. Hougan, D. Dignard, D. Y. Thomas, L. Bell, G. C. Saari, F. J. Grant, P. O'Hara, and V. L. MacKay.** 1989. The STE4 and STE18 genes of yeast encode potential β and γ subunits of the mating factor receptor-coupled G protein. Cell **56:**467–477.
71. **Yu, J.-H., J. Wieser, and T. H. Adams.** 1996. The *Aspergillus* FlbA RGS domain protein antagonizes G protein signaling to block proliferation and allow development. EMBO J. **15:**5184–5190.
72. **Zoller, M. J., and M. Smith.** 1984. Oligonucleotide-directed mutagenesis: a simple method using two oligonucleotide primers and a single-stranded DNA template. DNA **3:**479–488.